Hemocompatibility of Electrospun Halloysite Nanotube- and Carbon Nanotube-Doped Composite Poly(lactic-*co*-glycolic acid) Nanofibers

Yili Zhao,[1,2] Shige Wang,[3] Qingshan Guo,[4] Mingwu Shen,[5] Xiangyang Shi[1,5]

[1]Key Laboratory of Textile Science and Technology, Ministry of Education, Donghua University, Shanghai 201620, People's Republic of China
[2]College of Textiles, Donghua University, Shanghai 201620, People's Republic of China
[3]College of Materials Science and Engineering, Donghua University, Shanghai 201620, People's Republic of China
[4]Xinxiang Health School, Xinxiang 453000, People's Republic of China
[5]College of Chemistry, Chemical Engineering and Biotechnology, Donghua University, Shanghai 201620, People's Republic of China
Correspondence to: X. Shi (E-mail: xshi@dhu.edu.cn)

ABSTRACT: One of the major problems of nanofiber scaffold or other devices like cardiovascular or blood-contacting medical devices is their weak mechanical properties and the lack of hemocompatibility of their surfaces. In this study, halloysite nanotubes (HNTs) and carbon nanotubes (CNTs) were incorporated within poly(lactic-*co*-glycolic acid) (PLGA) nanofibers and the mechanical property and hemocompatibility of both types of composite nanofibers with different doping levels were thoroughly investigated. The morphology and internal distribution of the doped nanotubes within the nanofibers were characterized using scanning electron microscopy and transmission electron microscopy. Mechanical properties of the electrospun nanofibers were tested using a material testing machine. The hemocompatibility of the composite nanofibers was examined through hemolytic and anticoagulant assay, respectively. We show that the doped HNTs or CNTs are distributed in the nanofibers with a coaxial manner and the incorporation of HNTs or CNTs does not significantly change the morphology of the PLGA nanofibers. Importantly, the incorporation of HNTs or CNTs within PLGA nanofibers significantly improves the mechanical property of PLGA nanofibers, and PLGA nanofibers with or without doping of the HNTs and CNTs display good anticoagulant property and negligible hemolytic effect to human red blood cells. With the enhanced mechanical property, great hemocompatibility, and previously demonstrated biocompatibility of both HNTs- and CNTs-doped composite PLGA nanofibers, these composite nanofibers may be used as therapeutic artificial tissue/organ substitutes for tissue engineering applications. © 2012 Wiley Periodicals, Inc. J. Appl. Polym. Sci. 000: 000–000, 2012

INTRODUCTION

Electrospinning is an efficient way to produce nanofibers or microfibers with high surface area to volume ratio[1] for various applications, including but not limited to tissue engineering,[2–4] drug delivery systems,[5,6] biosensors,[7] environmental filtration membranes,[8–11] catalysis,[12] and sensitized solar cells.[13] In particular, the electrospun three-dimensional membranes possess high porosity, which is quite mimic to the natural extracellular matrix of human tissues. Therefore, electrospun nanofibers have a promising potential in substitution of a number of soft and hard tissues including vasculature, bone, neural, and tendon/ligament.[14]

Among many different classes of biodegradable polymers, poly-(lactic-*co*-glycolic acid) (PLGA) has received immense scientific and technological interests for biomedical applications due to their good biocompatibility and biodegradability.[15,16] For instance, PLGA has been used as scaffold materials for bone tissue engineering.[17] Porous PLGA scaffolds can be used to effectively repair mandibular defect of rabbits.[18] In a recent study, Lee et al. have successfully fabricated electrospun nanofiber scaffolds composed of PLGA and other polymers for vascular engineering applications.[19] With the great advantages of electrospun nanofibers, PLGA-based nanofibers should be useful for many different biomedical applications. Due to the weak mechanical property of PLGA polymer and the need for multifunctionality for practical tissue engineering applications, it is essential to modify PLGA nanofibers with enhanced mechanical property and desired functionality.[20]

In our previous work, we have shown that one-dimensional (1D) nanomaterials such as halloysite nanotubes (HNTs) ($Al_2Si_2O_5(OH)_4 \cdot nH_2O$)[4,6,21] and multiwalled carbon nanotubes (CNTs)[3,4,22] can be effectively incorporated within electrospun PLGA nanofibers. The incorporation of both HNTs and CNTs enables enhanced mechanical properties of the PLGA nanofibers.[21,22] In addition, compared with the PLGA nanofibers without incorporation of HNTs and CNTs, both HNTs- and CNTs-incorporated PLGA nanofibers appear to have a better protein adsorption capability, and display similar or better cell attachment and proliferation behaviors.[3,4,21] Furthermore, the HNTs-incorporated PLGA nanofibers can be used as drug carriers to allow efficient encapsulation and sustained release of drug molecules.[6] These studies suggest that HNTs- and CNTs-doped composite PLGA nanofibers may be used as new therapeutic artificial tissue/organ substitutes for tissue engineering applications.

For further biomedical applications of HNTs- and CNTs-doped composite PLGA nanofibers, hemocompatibility is becoming a key concern especially for the uses of these materials in contact with blood. In this study, electrospun HNTs- and CNTs-doped composite PLGA nanofibers were fabricated. The morphology of the nanofibers was characterized by scanning electron microscopy (SEM). The internal distribution of the doped nanotubes within the nanofibers was characterized by transmission electron microscopy (TEM), which has not been reported before. The hemocompatibility including hemolytic and anticoagulant assays of both HNTs- and CNTs-doped composite PLGA nanofibers with different doping levels was thoroughly investigated. To our knowledge, this is the first report related to the hemocompatibility evaluation of the 1D nanomaterial-containing PLGA nanofibers, which is very important for their further biomedical applications.

EXPERIMENTAL SECTION

Materials

PLGA (M_w = 81,000 gmol^{-1}) with a lactic acid : glycolic acid ratio of 50 : 50 was purchased from Jinan Daigang Biotechnology (Jinan, China). HNTs (diameter 75.8 ± 17.5 nm; length 445 ± 256 nm) were from Zhengzhou Jinyangguang China Clays (Zhengzhou, China). CNTs (diameter 30–70 nm; length 100–400 nm) with carboxyl residues were obtained according to previous reports.[23,24] Tetrahydrofuran (THF) and N, N-dimethyl formamide (DMF) were from Sinopharm Chemical Reagent (Shanghai, China). All the other chemicals were of analytical reagent grade and used as received. Water used in all experiments was purified using a Millipore Milli-Q Plus 185 water purification system (Millipore, Bedford, MA) with a resistivity higher than 18.2 MΩ cm.

Preparation of HNTs- and CNTs-Doped PLGA Nanofibers

HNTs- and CNTs-doped PLGA nanofibers were fabricated according to our previous work[4,21] but using a commercial electrospinning equipment (1006 Electrospinning equipment, Beijing Kang Sente Technology, Beijing, China). In brief, PLGA was dissolved in the mixed solvent of THF/DMF (v/v = 3 : 1) with a concentration of 25% (w/v). The use of the mixed solvent is able to generate PLGA and composite PLGA nanofibers with uniform fiber diameter distribution and smooth fiber morphol-

ogy, which has been demonstrated in our previous work.[21,22] Before electrospinning, different amounts of HNTs or CNTs (1, 3, and 5 wt % relative to PLGA, respectively) were mixed with PLGA solution, and sonicated for 30 min. The applied voltage and collection distance were set as 20 kV and 15 cm, respectively. The flow rate of 0.8 mLh^{-1} was controlled by a syringe pump, and the inner spinneret diameter was 1.0 mm. The needle and collector were set in a vertical direction. The humidifier and temperature control system in the electrospinning equipment were used to maintain the humidity to be in a range of 40–50% and the temperature in the range of 20–25°C, respectively. The formed HNTs- and CNTs-doped composite PLGA nanofibers were dried in vacuum oven for at least two days to remove the residual organic solvent and moisture.

Characterization Techniques

The morphology of electrospun nanofibers was observed using SEM (JEOL JSM-5600LV, Japan). The accelerating voltage was set at 15 kV. Before SEM observations, the samples were sputter coated with gold films with a thickness of 10 nm. The diameters of the electrospun fibers were analyzed using ImageJ 1.40G software (http://rsb.info.nih.gov/ij/download.html, National Institutes of Health, USA). At least 100 nanofibers randomly selected from different images were analyzed for each sample. TEM samples of HNTs- and CNTs-doped PLGA nanofibers were prepared by collecting electrospun fibers onto carbon-coated copper grid attached onto the collector. TEM was performed using a Hitachi H-800 transmission electron microscope (Tokyo, Japan) with a voltage of 200 kV. Mechanical properties of the electrospun nanofibers were tested using a material testing machine (H5K-S, Hounsfield, UK) at the temperature of 20°C and humidity of 63%. The fiber samples were cut into rectangular pieces with an area of 10 × 50 mm^2 before testing. The cross-head speed was set to be 10 mmmin^{-1}. The stress and strain data were calculated using eqs. (1) and (2):

$$\sigma(\text{MPa}) = \frac{P(N)}{w(\text{mm}) \times d(\text{mm})} \quad (1)$$

$$\varepsilon = \frac{l}{l_0} \times 100\% \quad (2)$$

Where σ, ε, P, w, d, l, and l_0 stand for stress, strain, load, mat width, mat length, extension length, and gauge length, respectively. Breaking strength, failure strain, and Young's modulus were obtained from the strain-stress curves.

Hemolytic Assay

Human blood stabilized with heparin was kindly provided by Shanghai First People's Hospital (Shanghai, China). Then the blood was centrifuged and washed with phosphate buffer saline (PBS) five times according to the procedure reported in literature[25,26] to completely remove serum and obtain human red blood cells (HRBCs). After that, the HRBCs were diluted 10 times with PBS solution. Then, 0.2 mL of the diluted HRBCs suspension was transferred to a 1.5-mL Eppendorf tube which was filled with 0.8 mL of water (as positive control) and PBS buffer (as negative control), respectively. Nanofibrous samples and HNTs or CNTs powders (2 mg) were exposed to 1.0 mL HRBCs suspension containing 0.2 mL diluted HRBCs
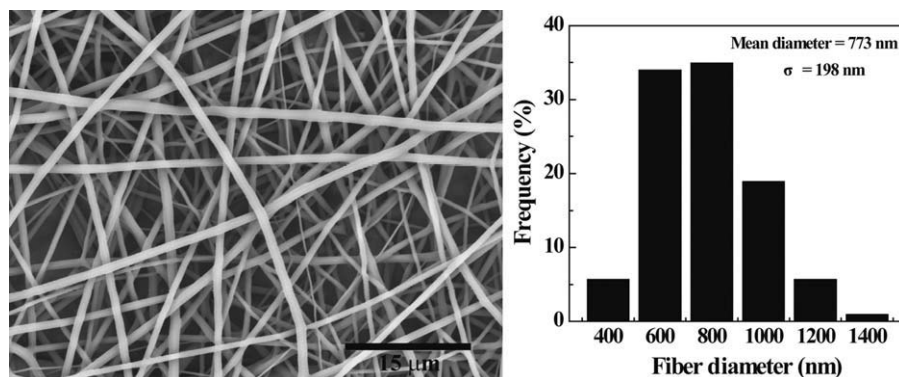
Figure 1. SEM micrograph and diameter distribution histogram of PLGA nanofibers.

suspension and 0.8 mL PBS buffer, respectively. The above mixtures were then incubated at 37°C for 2 h, followed by centrifugation (10,000 rpm; 2 min). Then the supernatant was deter-

mined by Perkin Elmer Lambda 25 UV–vis spectrometer to record the absorbance at 540 nm. The hemolytic percentage (HP) was calculated using eq. (3).[27,28]
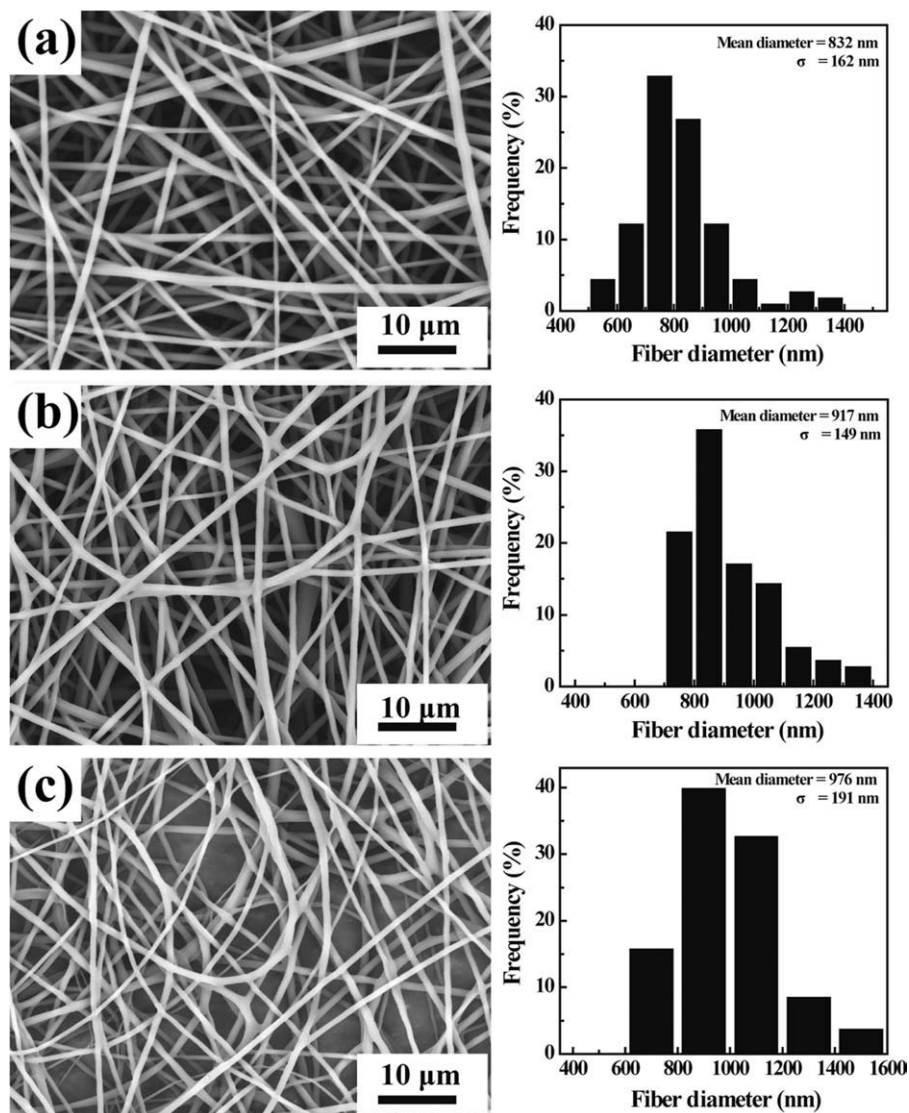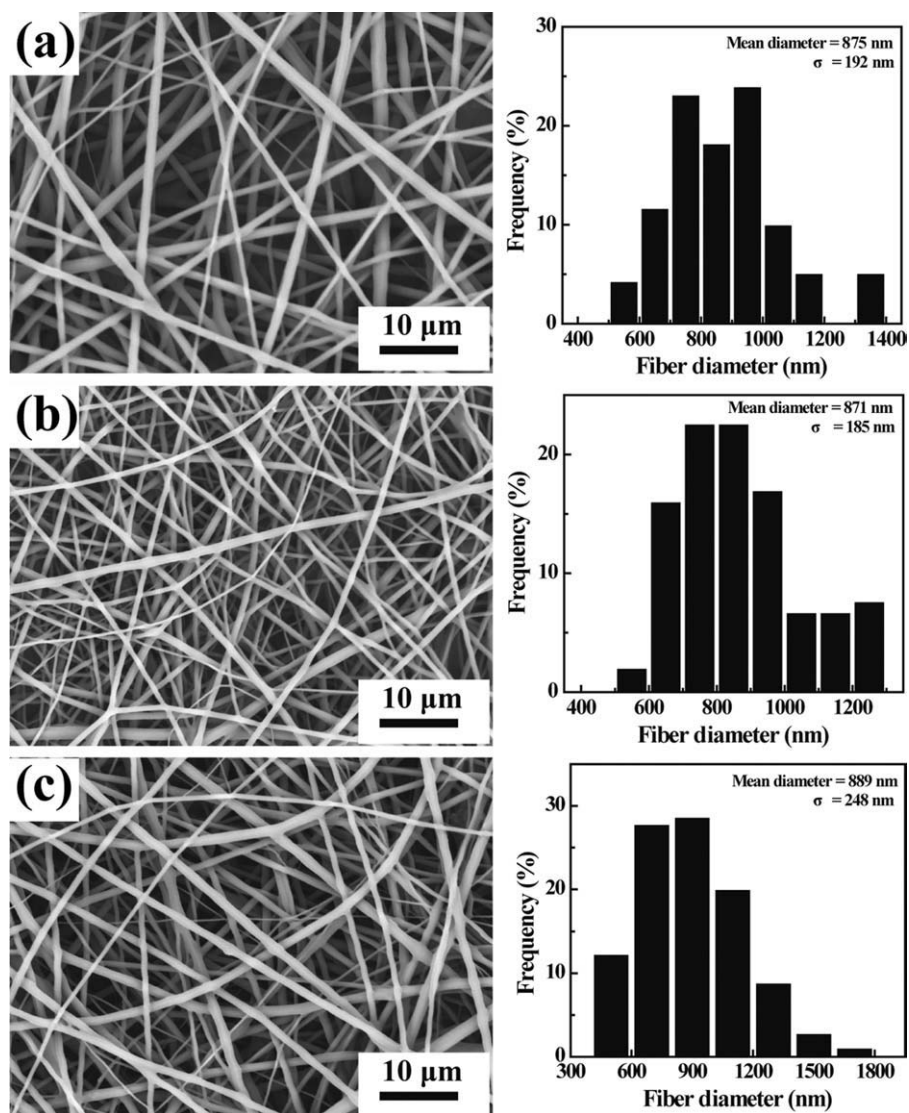

Figure 2. SEM micrographs and diameter distribution histograms of HNTs-doped PLGA nanofibers with (a) 1%, (b) 3%, and (c) 5% HNTs relative to PLGA, respectively.

Figure 3. SEM micrographs and diameter distribution histograms of CNTs-doped PLGA nanofibers with (a) 1%, (b) 3%, and (c) 5% CNTs relative to PLGA, respectively.

$$HP(\%) = \frac{(D_t - D_{nc})}{(D_{pc} - D_{nc})} \times 100\% \quad (3)$$

where D_t is the absorbance of the test sample; D_{pc} and D_{nc} are the absorbance of the positive and negative control, respectively.

Anticoagulant Assay

The anticoagulant properties of the nanofiber samples with a dimension of 20×20 mm^2 were determined by a kinetic clotting time method described in the previous studies.[29–31] In brief, the as-prepared nanofibrous mats were cut into small pieces in a dimension of 20×20 mm^2 in triplicate and were put into individual well of 12-well tissue culture plate. Cover slips without nanofibers were used as control. Then, fresh human blood (20 μL) was dropped onto the surface of the nanofibrous samples and the cover slips, respectively, followed by adding 10 μL of CaCl$_2$ solution (0.2 molL^{-1}) to each blood drop and incubating at 37°C for a predetermined period of time (5, 10, 20, 40, and 60 min). After that, 5 mL water was put into each well carefully and incubated at 37°C for 5 min. The concentration of hemoglobin in water was measured by
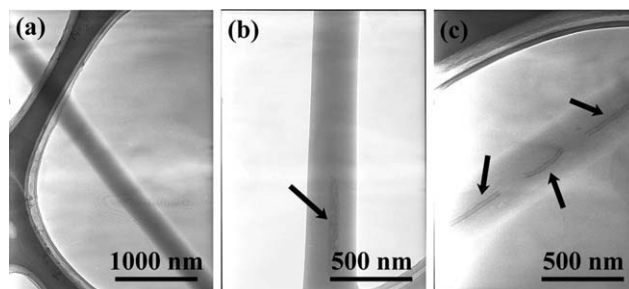
Figure 4. TEM micrographs of (a) PLGA nanofibers, (b) HNTs-doped PLGA nanofibers with 5% HNTs relative to PLGA, and (c) CNTs-doped PLGA nanofibers with 5% CNTs relative to PLGA. The arrows indicate the nanotubes embedded within the PLGA nanofibers.
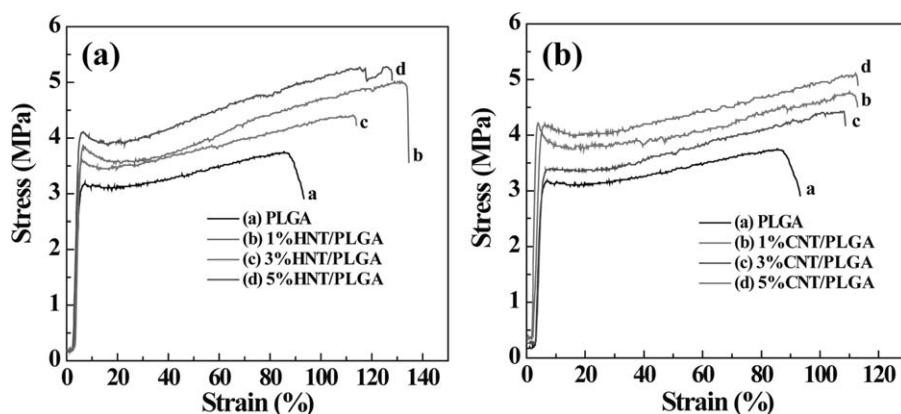
Figure 5. Strain-stress curves of (a) HNTs- and (b) CNTs-doped PLGA nanofibers.

monitoring the absorbance at 540 nm using a Lambda 25 UV–vis spectrophotometer (Perkin Elmer).

Statistical Analysis

One way ANOVA statistical analysis was performed to compare the HP of different materials. The P value of 0.05 was selected as the significance level.

RESULTS AND DISCUSSION

Characterization of the Electrospun Composite Nanofibers

The primary goal of this work is to demonstrate that the incorporated HNTs and CNTs in the nanofibers are able to enhance the mechanical properties of the fibers without compromising the hemocompatibility of the PLGA nanofibers. In addition, our previous work has shown that the incorporation of HNTs or CNTs in the PLGA nanofibers appears to have a better protein adsorption capability, and display similar or better cell attachment and proliferation behaviors.[3,21] Likewise, our previous work has shown that HNTs/PLGA nanofibers can be used as drug carriers to allow efficient encapsulation and sustained release of drug molecules, greatly reducing the burst release of the drug.[6] With the drug carrier application of CNTs,[32,33] the developed CNTs-doped PLGA nanofibers could also be used as an efficient drug delivery system.

The morphology of PLGA and composite PLGA nanofibers was observed by SEM. Figure 1 shows a typical SEM image of the PLGA nanofibers without doping of HNTs or CNTs. It is clear that the PLGA nanofibers have a smooth surface and relatively uniform fiber diameter distribution with a mean diameter of

773 nm. When doped with different levels of HNTs and CNTs, the morphology of PLGA nanofibers does not significantly change when compared with PLGA nanofibers without doping of the nanotubes, except that the mean diameter increases with the doping level of HNTs (Figure 2) or CNTs (Figure 3). From Figure 2, we can see that the diameters of HNTs-doped PLGA nanofibers with doping level of 1, 3, and 5 wt % HNTs relative to PLGA are 832, 917, and 976 nm, respectively. Similarly, from Figure 3, it can be seen that the diameters of the CNTs-doped PLGA nanofibers with 1, 3, and 5 wt % CNTs relative to PLGA are 875, 871, and 889 nm, respectively. The slightly larger diameter of PLGA or composite PLGA nanofibers incorporated with the corresponding levels of HNTs or CNTs than that reported in our previous work[4] may be due to the use of different electrospinning equipments. The fiber diameter generally increases with the increase of the incorporation percentage of HNTs or CNTs. The incorporation of negatively charged HNTs or CNTs into the PLGA solution may result in a decrease of the surface charge density of the spinning jet, leading to the formation of nanofibers with a larger diameter, in agreement with literature.[34]

The distribution and alignment of the incorporated HNTs or CNTs inside the PLGA nanofibers were confirmed by TEM imaging (Figure 4). At the loading level of 5%, HNTs and CNTs appear to be well embedded in the PLGA fiber matrix and highly oriented along the fiber axis, in agreement with results reported in literature.[35] In contrast, no nanotubes can be observed inside the pure PLGA nanofibers. The coaxial alignment of HNTs or CNTs within PLGA nanofibers may be

Table I. Tensile Properties of Electrospun PLGA Nanofibers and Composite PLGA Nanofibers Doped with HNTs Under the Same Processing Conditions

Sample	Breaking strength (MPa)	Failure strain (%)	Young's modulus (MPa)
PLGA	3.94 ± 0.49	89.60 ± 13.45	66.53 ± 14.76
HNTs(1%)-PLGA	4.74 ± 0.52	117.40 ± 21.87	87.67 ± 22.06
HNTs(3%)-PLGA	4.28 ± 0.37	91.76 ± 17.84	94.51 ± 11.82
HNTs(5%)-PLGA	4.76 ± 0.33	118.84 ± 15.71	93.35 ± 8.85

Data are representative of independent experiments and all data are given as mean ± SD; $n = 5$.

Table II. Tensile Properties of Electrospun PLGA Nanofibers and Composite PLGA Nanofibers Doped with CNTs Under the Same Processing Conditions

Sample	Breaking strength (MPa)	Failure strain (%)	Young's modulus (MPa)
PLGA	3.94 ± 0.49	89.60 ± 13.45	66.53 ± 14.76
CNTs(1%)-PLGA	4.76 ± 0.37	103.81 ± 38.27	99.22 ± 41.82
CNTs(3%)-PLGA	4.19 ± 0.37	90.84 ± 4.87	85.70 ± 18.75
CNTs(5%)-PLGA	4.82 ± 0.29	90.26 ± 14.3	93.83 ± 26.39

Data are representative of independent experiments and all data are given as mean ± SD; $n = 5$.

because of the particle-particle interactions of the nanotubes can be overcome by the elongation and shear force during the electrospinning process.[36]

The incorporation of HNTs or CNTs within PLGA nanofibers significantly improved the mechanical property of PLGA nanofibers (Figure 5). Tables I and II list the detailed mechanical parameters of all fiber samples. Apparently, the breaking strength, failure strain, and Young's modulus of the HNTs- or CNTs-doped PLGA nanofibers were all enhanced when compared with those of PLGA nanofibers without doping of HNTs or CNTs. The improved mechanical property should be due to the fact that the external load can be efficiently transferred from the PLGA matrix to the doped CNTs or HNTs, in agreement with our previous work.[21,22] It is worthwhile to note that the loading of HNTs or CNTs with different percentages (1–5%) within the PLGA nanofibers leads to slight changes in the mechanical parameters, suggesting that the mechanical load transfer from PLGA matrix to the nanotubes is not very sensitive to the loading percentage of the HNTs or CNTs within a range of 1–5%. These data are different from those reported in our previous

work,[21] which may be due to the fact that the nanofibers were formed using different electrospinning instruments and therefore had different fiber diameter and morphology. We also note that although the dimension of HNTs (diameter 75.8 ± 17.5 nm; length 445 ± 256 nm) and CNTs (diameter 30–70 nm; length 100–400 nm) is quite different, both nanotubes are able to enhance the mechanical properties of PLGA nanofibers in a more or less similar way and similar folds in terms of their mechanical parameters (except for the failure strain data) under similar doping percentages. This could be because of the load transfer from PLGA matrix to the nanotubes is not sufficiently sensitive to the differences of the type and dimension of the nanotubes.

Hemolytic Effect of Electrospun Composite PLGA Nanofibers

For applications in therapeutic artificial tissue/organ substitutes, one main concern of the fibrous materials is their potency of hemolysis when contacting blood.[37,38] In this study, we thoroughly investigated the hemocompatibility of PLGA, and HNTs- or CNTs-doped composite PLGA nanofibers with different doping levels. The HNTs and CNTs powders were also tested as controls.
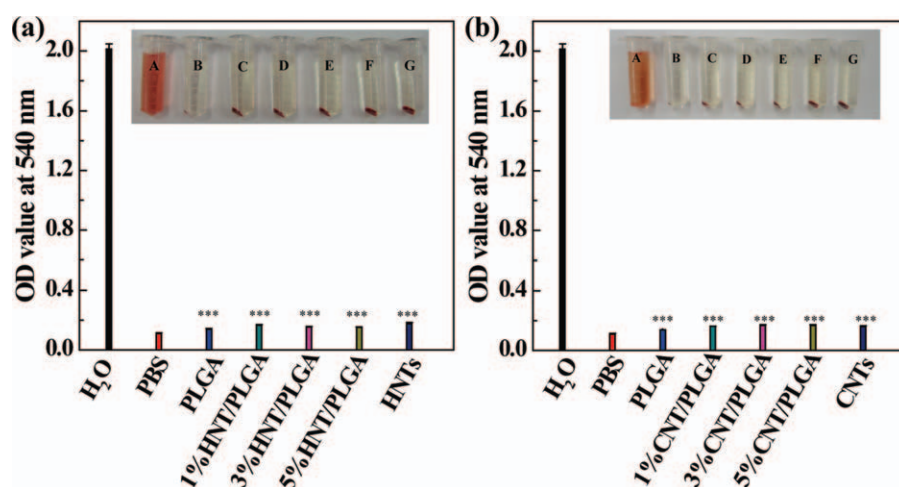
Figure 6. Hemolytic assay of (a) HNTs- and (b) CNTs-doped PLGA nanofibers. The inset of (a) shows a photograph of HRBCs exposed to (A) water, (B) PBS solution, (C) PLGA nanofibers, (D) HNTs-doped PLGA nanofibers (1% HNTs relative to PLGA), (E) HNTs-doped PLGA nanofibers (3% HNTs relative to PLGA), (F) HNTs-doped PLGA nanofibers (5% HNTs relative to PLGA), and (G) HNTs powder, followed by centrifugation. The inset of (b) shows a photograph of HRBCs exposed to (A) water, (B) PBS solution, (C) PLGA nanofibers, (D) CNTs-doped PLGA nanofibers (1% CNTs relative to PLGA), (E) CNTs-doped PLGA nanofibers (3% CNTs relative to PLGA), (F) CNTs-doped PLGA nanofibers (5% CNTs relative to PLGA), and (G) CNTs powder, followed by centrifugation. Statistical differences between nanofiber or powder samples versus the negative control (water) were compared and indicated with (*) for $P < 0.05$, (**) for $P < 0.01$, and (***) for $P < 0.001$, respectively. [Color figure can be viewed in the online issue, which is available at wileyonlinelibrary.com.]

Table III. Hemolysis Percentage (HP) of PLGA Nanofibers and Composite PLGA Nanofibers Doped with HNTs in Comparison with HNTs Powder

Samples	PLGA	HNTs(1%)-PLGA	HNTs(3%)-PLGA	HNTs(5%)-PLGA	HNTs powder
HP (%)	1.5	3.0	2.4	2.2	3.5

Table IV. Hemolysis Percentage (HP) of PLGA Nanofibers and Composite PLGA Nanofibers Doped with CNTs in Comparison with CNTs Powder

Samples	PLGA	CNTs(1%)-PLGA	CNTs(3%)-PLGA	CNTs(5%)-PLGA	CNTs powder
HP (%)	1.5	2.7	3.0	3.1	2.7

As can be seen in insets of Figure 6(a, b), after exposure of all fiber samples and the HNTs or CNTs powers to the solution of HRBCs solution, no obvious hemolytic phenomenon can be observed except the negative control (water). The hemolytic effect of each material was further quantified by recording the absorbance of the supernatant at 540 nm using UV–vis spectroscopy. It is clear that there is significant difference ($P < 0.001$) in the absorbance at 540 nm associated with hemoglobin between the positive control group (HRBCs exposed to water) and the experimental groups. The hemolysis percentage of PLGA nanofibers, HNTs- and CNTs-doped PLGA nanofibers (1, 3, and 5 wt % relative to PLGA, respectively), and HNTs or CNTs powder calculated by eq. (3) were all <5% (Tables III and IV), indicating that the studied materials do not display appreciable hemolytic effect.[39]

Anticogulation of Electrospun Composite PLGA Nanofibers
The coagulation of the blood is initiated by thrombin that transforms fibrinogen into fibrin monomers, which under normal conditions form polymeric fibrin fibers, resulting in a clot network.[40] Therefore, to evaluate the applicability of a biomaterial to be used in contact with blood, it is important to investigate the blood clotting behavior of the material. Figure 7 shows the optical density (OD) values of haemoglobin at 540 nm of the supernatant when incubated on different materials under the predetermined time intervals. A higher OD value represents a higher hemoglobin concentration and suggests that the clotting behavior of the material is less obvious. The OD values of the PLGA, HNTs-, and CNTs-doped composite PLGA nanofibers are relatively higher at each time point than those on glass

cover slips, in agreement with literature.[31] In addition, there is no significant difference in the OD values ($P > 0.05$) between the pure PLGA and samples of different content of incorporated HNTs or CNTs at different time points. This may be due to the fact that the HNTs or CNTs are well incorporated within the PLGA nanofibers, and the surface property of composite PLGA nanofibers doped with different levels of HNTs or CNTs does not have appreciable changes when compared with that of the PLGA nanofibers without doping. In contrast, under similar experimental conditions, glass cover slips display significant clotting behavior after incubation for 60 min, the absorbance of hemoglobin in the case of cover slip is 0.11, much lower than those of the fibrous samples (the lowest value of 0.25 at 60 min for 1% CNT/PLGA fibers). These results imply that all the PLGA fibrous mats with or without doping of HNTs or CNTs possess good anticoagulant property.

CONCLUSION

In summary, electrospun HNTs- and CNTs- doped PLGA nanofibers were fabricated and their hemocompatibility have been thoroughly investigated. We show that the doping of HNTs or CNTs does not significantly impact the smooth morphology of PLGA nanofibers except the change of fiber diameter and the 1D nanomaterial is distributed within the nanofibers in a coaxial manner. The incorporation of both types of nanotubes enables enhanced mechanical properties of the PLGA nanofibers. The lower HP (<5%) in the hemolysis assay for all the fibrous materials and the higher OD values of the hemoglobin in
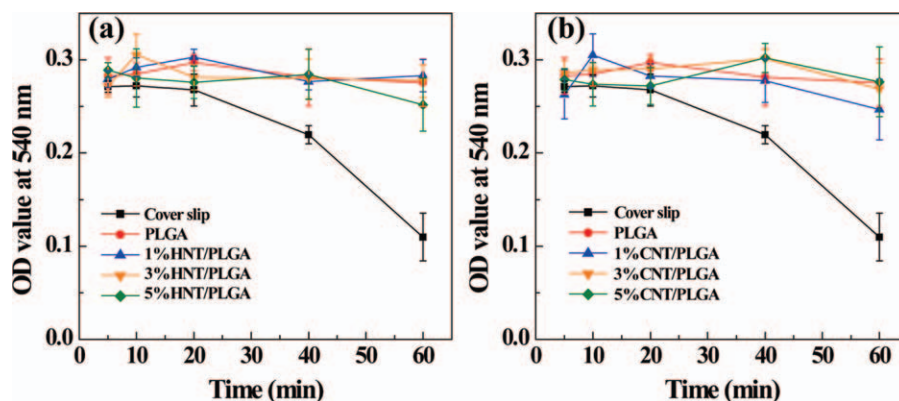
Figure 7. Anticoagulant assay of (a) HNTs- and (b) CNTs-doped PLGA nanofibers at different time intervals. [Color figure can be viewed in the online issue, which is available at wileyonlinelibrary.com.]

the anticoagulant assay for all the fibrous materials when compared with those of cover slips indicate that the PLGA nanofibers with or without doping of HNTs or CNTs display good hemocompatibility. This suggests that the doping of PLGA nanofibers with the two types of nanotubes at the given doping percentages does not significantly alter the surface properties of PLGA nanofibers. With the good hemocompatibility and the previously demonstrated good biocompatibility of the HNTs- or CNTs-incorporated PLGA nanofibers, these fibrous materials may be readily used as therapeutic artificial tissue/organ substitutes for tissue engineering applications.

ACKNOWLEDGMENTS

REFERENCES

1. Theron, S. A.; Zussman, E.; Yarin, A. L. *Polymer* **2004,** *45*, 2017.

2. Pham, Q. P.; Sharma, U.; Mikos, A. G. *Tissue. Eng.* **2006,** *12*, 1197.

3. Liu, F. J.; Guo, R.; Shen, M. W.; Cao, X. Y.; Mo, X. M.; Wang, S. Y.; Shi, X. Y. *Soft Mater.* **2010,** *8*, 239.

4. Qi, R.; Shen, M.; Cao, X.; Guo, R.; Tian, X.; Yu, J.; Shi, X. *Analyst* **2011,** *136*, 2897.

5. Kenawy, E. R.; Abdel-Hay, F. I.; El-Newehy, M. H.; Wnek, G. E. *Mater. Chem. Phys.* **2009,** *113*, 296.

6. Qi, R.; Guo, R.; Shen, M.; Cao, X.; Zhang, L.; Xu, J.; Yu, J.; Shi, X. J. *Mater. Chem.* **2010,** *20*, 10622.

7. Li, D.; Frey, M. W.; Baeumner, A. J. *J. Membr. Sci.* **2006,** *279*, 354.

8. Fang, X.; Xiao, S.; Shen, M.; Guo, R.; Wang, S.; Shi, X. *New J. Chem.* **2011,** *35*, 360.

9. Xiao, S.; Ma, H.; Shen, M.; Wang, S.; Huang, Q.; Shi, X. *Colloids Surf. A* **2011,** *381*, 48.

10. Xiao, S.; Shen, M.; Guo, R.; Huang, Q.; Wang, S.; Shi, X. J. *Mater. Chem.* **2010,** *20*, 5700.

11. Xiao, S.; Shen, M.; Guo, R.; Wang, S.; Shi, X. *J Phys. Chem. C* **2009,** *113*, 18062.

12. Fang, X.; Ma, H.; Xiao, S.; Shen, M.; Guo, R.; Cao, X.; Shi, X. J. *Mater. Chem.* **2011,** *21*, 4493.

13. Thavasi, V.; Singh, G.; Ramakrishna, S. *Energy Environ. Sci.* **2008,** *1*, 205.

14. Sill, T. J.; Von Recum, H. A. *Biomaterials* **2008,** *29*, 1989.

15. Agrawal, C.; Ray, R. B. *J Biomed. Mater. Res.* **2001,** *55*, 141.

16. Jain, R. A. *Biomaterials* **2000,** *21*, 2475.

17. Karp, J. M.; Shoichet, M. S.; Davies, J. E. *J. Biomed. Mater. Res.* **2003,** *64*, 388.

18. Ren, T.; Ren, J.; Jia, X.; Pan, K. J. *Biomed. Mater. Res.* **2005,** *74*, 562.

19. Lee, S. J.; Yoo, J. J.; Lim, G. J.; Atala, A.; Stitzel, J. J. *Biomed. Mater. Res.* **2007,** *83*, 999.

20. Butler, D. L.; Goldstein, S. A.; Guilak, F. J. *Biomech. Eng. Trans. ASME* **2000,** *122*, 570.

21. Qi, R.; Cao, X.; Shen, M.; Guo, R.; Yu, J.; Shi, X. J. *Biomater. Sci. Polym. Ed.* **2012,** *23*, 299.

22. Liu, F.; Guo, R.; Shen, M.; Wang, S.; Shi, X. *Macromol. Mater. Eng.* **2009,** *294*, 666.

23. Petersen, E. J.; Huang, Q.; Weber, J. W. *J. Environ. Sci. Technol.* **2008,** *42*, 3090.

24. Petersen, E. J.; Huang, Q.; Weber W. J., Jr. *Environ. Health. Perspect.* **2008,** *116*, 496.

25. Hu, H.; Zhou, H.; Du, J.; Wang, Z.; An, L.; Yang, H.; Li, F.; Wu, H.; Yang, S. J. *Mater. Chem.* **2011,** *21*, 6576.

26. Wu, H.; Liu, G.; Zhuang, Y.; Wu, D.; Zhang, H.; Yang, H.; Hu, H.; Yang, S. *Biomaterials* **2011,** *32*, 4867.

27. He, Q.; Zhang, J.; Shi, J.; Zhu, Z.; Zhang, L.; Bu, W.; Guo, L.; Chen, Y. *Biomaterials* **2010,** *31*, 1085.

28. Lin, Y. S.; Haynes, C. L. *Chem. Mater.* **2009,** *21*, 3979.

29. Imai, Y.; Nose, Y. J. *Biomed. Mater. Res.* **1972,** *6*, 165.

30. Lee, K. Y.; Ha, W. S.; Park, W. H. *Biomaterials* **1995,** *16*, 1211.

31. Meng, Z. X.; Zheng, W.; Li, L.; Zheng, Y. F. *Mater. Sci. Eng. C* **2010,** *30*, 1014.

32. Ali-Boucetta, H.; Al-Jamal, K. T.; McCarthy, D.; Prato, M.; Bianco, A.; Kostarelos, K. *Chem. Commun.* **2008,** 459.

33. Liu, Z.; Sun, X.; Nakayama-Ratchford, N.; Dai, H. *ACS Nano.* **2007,** *1*, 50.

34. Fong, H.; Chun, I.; Reneker, D. *Polymer* **1999,** *40*, 4585.

35. Zhang, Q.; Chang, Z.; Zhu, M.; Mo, X.; Chen, D. *Nanotechnology* **2007,** *18*, 115611.

36. Yang, T.; Wu, D.; Lu, L.; Zhou, W.; Zhang, M. *Polym. Compos.* **2011,** *32*, 1280.

37. Dey, R. K.; Ray, A. R. *Biomaterials* **2003,** *24*, 2985.

38. Shim, D.; Wechsler, D. S.; Lloyd, T. R.; Beekman, R. H., III. *Cathet. Cardiovasc. Diagn.* **1996,** *39*, 287.

39. Wang, Q. Z.; Chen, X. G.; Li, Z. X.; Wang, S.; Liu, C. S.; Meng, X. H.; Liu, C. G.; Lv, Y. H.; Yu, L. J. *J. Mater. Sci.: Mater. Med.* **2008,** *19*, 1371.

40. Smith, B. S.; Yoriya, S.; Grissom, L.; Grimes, C. A.; Popat, K. C. *J. Biomed. Mater. Res.* **2010,** *95*, 350.